IAC-26-B2-8-GTS.3-1-x107031

A New Generation Commercial Data Relay Satellite System

Liyan Zhang[a]*, **Bo Li**[ab], **Changgang Zheng**[c]*

[a] *Cangyu Space, Beijing, China*
[b] *Beijing University of Posts and Telecommunications, Beijing, China*
[c] *Nanjing University, Nanjing, China*

* Corresponding Author

Abstract

Data relay satellite systems have played a critical role in ensuring continuous tracking, telemetry, and command (TT&C) support and high-rate data transmission for crewed missions and Earth observation satellites since the 1960s. With the rapid expansion of commercial space activities, including large scale LEO constellations, high-resolution remote sensing satellites, lunar exploration missions, and emerging space tourism, existing relay architectures face significant challenges in scalability, cost efficiency, flexible access, and service diversity. Based on the analysis of user requirements, e.g., application scenarios, service performance, and service models, as well as system construction constraints, this paper proposes a new-generation commercial data relay satellite system based on an Inclined Geosynchronous Orbit (IGSO) constellation architecture. Compared with traditional GEO-based relay systems, the IGSO configuration improves launch mass efficiency, reduces the consumption of propellant required for long-term position maintenance, and still enables wide-area coverage. The architecture integrates onboard S/X-band TT&C panoramic antennas to support rapid, on-demand TT&C access and emergency communication for conventional spacecraft users, enabling flexible and scalable service provisioning. The system adopts a microwave and laser hybrid payload architecture, addressing heterogeneous data transmission requirements. Microwave links provide robust and cost-effective medium-range services, while large-aperture optical payloads enable high-rate and long-range data relay, particularly for lunar missions and deep-space exploration scenarios. In addition, the system design incorporates intelligent resource scheduling, flexible pricing strategies, and ecosystem collaboration mechanisms to support large-scale commercial users, including LEO communication constellations and crewed spacecraft requiring full TT&C coverage for safety assurance. Analysis shows that the proposed architecture can serve as a low-cost, highly available, and commercially sustainable relay infrastructure, supporting the next phase of Earth orbital activities, lunar development, and deep-space exploration.

Keywords: Commercial Data Relay Satellite System, IGSO Constellation, Space–Ground Integrated Network, Massive Multi-User Access, Microwave–Laser Hybrid Relay

1. Introduction

Early satellite TT&C mainly relied on ground stations. Because of Earth curvature and the line-of-sight propagation of radio waves, a single ground station covers only about 2–3% of a LEO spacecraft orbit [1, 2]. More than 100 ground stations would be required worldwide to provide 100% TT&C coverage for a spacecraft at an altitude of 300 km, resulting in substantial construction difficulty and cost. The concept of space-based TT&C, as an alternative, emerged, and major spacefaring nations have successively developed multiple satellite data relay systems.

The United States has developed three generations of Tracking and Data Relay Satellites (TDRS) [3]. Their inter-satellite link frequency has evolved from Ku-band to Ka-band, the single-access link data rate has increased to 800 Mbps, and the forward and return data rates for multiple-access data relay have reached 300 Kbps and 3 Mbps, respectively. In 2021, the United States proposed the Communication Services Project (CSP), which aims to provide more flexible services at lower cost [4]. By reusing mature constellation resources, it has begun to form a commercial relay service system integrating GEO, MEO, and LEO assets. Russia operates a globally covering relay satellite system that provides data relay and fixed communication services using Ku-band and S-band 4.2 m antennas and multiple omnidirectional helical antennas [5]. The European Space Agency developed the European Data Relay System (EDRS), the world's first commercial high-orbit laser relay system, which provides 1.8 Gbps laser data transmission services for LEO spacecraft [6]. In 2022, ESA released Infrastructure for Resilience, Interconnectivity and Security by Satellite ($IRIS^2$), and under its framework developed next-generation relay communication system with a hybrid high/low-orbit network reusing EDRS high-orbit assets [7]. Japan launched Japanese Data Relay System-1 (JDRS-1) in 2020, providing S/Ka-band data transmission and 1.8 Gbps laser data relay [8, 9]. The Canadian commercial company Kepler completed the deployment and initial commercial operation of its first ten all-optical relay satellites in 2024 and plans to build an 18-satellite dedicated network for all-optical data relay and on-orbit computing services by 2028 [10]. China has developed three generations of high-orbit relay satellites [11]; multiple satellites across these generations can operate cooperatively for global coverage, support simultaneous access by dozens of targets, and provide data rates up to 1.2 Gbps. Queqiao-1, operating near the Earth–Moon L2 point, provides far-side lunar relay through a 4.2 m X-band antenna [12], while Queqiao-2, operating in near-rectilinear halo orbit (NRHO), provides up to 500 Mbps relay services for the whole Moon, especially the south polar region, through a 0.6 m S/Ka-band parabolic antenna [13]. In recent years, several private companies have also begun building and operating commercial relay constellations in high or medium orbits.

A review of the history of data relay satellite systems and the trend of human space activities indicates the following developments.

First, application scenarios and functional-performance requirements are becoming more diverse and more demanding. Massive satellite health monitoring and emergency control require relay systems to respond immediately to concurrent low-rate TT&C and telemetry return requests from many users. Remote sensing service-data return and video and voice transmission for crewed missions require higher-rate and more reliable data transmission. Deep-space exploration requires an integrated Earth–Moon space infrastructure that supports communications, navigation, positioning, and timing over longer distances. Future relay satellite systems should therefore serve more users simultaneously, support on-demand access, provide higher transmission rates, and cover both near-Earth and cislunar space.

Second, two technical paths coexist: high-orbit satellites and LEO constellations. LEO relay can reuse high-speed broadband inter-satellite links in internet constellations or low-rate narrowband data links in Internet of Things constellations. It offers low latency, low path loss, high data rates, and a market scale that grows rapidly with constellation deployment, but it still faces challenges in inter-satellite link stability and dynamic constellation control. Conventional high-orbit relay has wide coverage, mature technology, and stable links, but it also has higher transmission latency, smaller single-link bandwidth, and scarce orbital-slot resources. A multi-orbit integrated architecture, serving different user classes through a coordinated ecosystem, is expected to become a key trend in future space-based relay systems.

Third, commercial participation is accelerating. Under the U.S. CSP, relay services that reuse on-orbit resources such as Starlink LEO broadband constellations [14], SES O3b mPOWER MEO communication constellations [15], and Viasat GEO high-throughput satellites have rapidly developed capability and entered commercial operation [16]. ESA-led EDRS and $IRIS^2$ are both operated through public–private partnerships, with Airbus Defence and Space, Thales Alenia Space, SES, and other companies participating in $IRIS^2$ [6, 7]. In China, while the Tianlian system continues to serve major national space projects [17], a new commercial space-based relay market has emerged, with companies building high-orbit or MEO relay constellations and providing services based on IoT constellations.

In summary, countries have built relay satellite systems matched to the space missions of their time. However, as humanity enters an era of large-scale space activity [18–24], existing systems cannot effectively meet current and future mission needs. The rapid development of commercial spaceflight has also created strong demand for space-based data relay services that exceeds available supply. A new-generation commercial relay satellite system is needed to fill the market gap. Based on current satellite data relay requirements, aerospace technology trends, and representative application scenarios, this paper proposes a commercial relay satellite system concept using a high-orbit relay technical path and presents a top-level design for its performance, architecture, operational regime, and application model.

2. Requirements and Functional Positioning

The era of large-scale space activity imposes new requirements and challenges on the function, performance, application model, construction, and operation of relay satellite systems. Accurate user-demand positioning and differentiated high-quality service for specific market segments are the basis for building a commercial relay satellite system.

2.1 User Requirement Analysis

Basic TT&C requirements for massive users. The primary task of TT&C is to ensure spacecraft safety under all operating conditions, including all flight phases and abnormal attitudes such as tumbling. A new-generation relay satellite system should provide omnidirectional coverage links for diverse users and meet the needs of real-time health monitoring and emergency response during failures.
High-rate real-time data transmission. The explosive growth in the number of on-orbit satellites has sharply increased data transmission demand. Higher frequency bands and wider bandwidths are needed to establish bidirectional high-rate inter-satellite and space-to-ground data channels. Payload design must also coordinate with user terminals and ground systems to support on-demand access and immediate return of satellite service data.
Data relay for deep-space exploration. The Moon is becoming a new commercial focus, and Earth–Moon transport and lunar activities require reliable TT&C and data transmission support. A new-generation relay system should serve as a data transfer station for lunar missions, providing bidirectional TT&C and communication links with Earth for probes in Earth–Moon transfer, lunar descent, and lunar orbit, as well as for lunar rovers, lunar-surface spacecraft, and astronaut surface activities.
Feeder-link bandwidth bottleneck. Radio-frequency feeder links in space-based TT&C systems becomes a new bottleneck in connecting space and ground. When large volumes of user data are returned through concentrated nodes, greater space-to-ground spectrum bandwidth is required. An integrated and coordinated space–ground data connectivity network must therefore be built under International Telecommunication Union (ITU) regulatory constraints.
Commercial service requirements. Reliable and low-cost data relay services require coordinated consideration of technical advancement, system reliability, and construction and operation costs. The system should maximize infrastructure reuse, expand diversified service capabilities, guide user adoption, and provide commercial services through market-oriented operation.

For these typical application scenarios and commercial service requirements, the new-generation commercial relay satellite system is positioned to provide low-rate TT&C services for massive LEO spacecraft, medium- and high-rate real-time service-data transmission for LEO spacecraft such as remote sensing constellations, and data transfer services for Earth–Moon transfer and lunar or other deep-space missions, as well as cataloging of civil and commercial spacecraft of medium- and low-orbit and space traffic management services such as collision warning based on cataloging.

2.2 Definition of Functions and Performance

Based on this positioning, the system should provide basic TT&C communication support under any operating condition, at any location, and at any time, meeting the core needs of routine status monitoring and rapid emergency rescue; return high-rate satellite service data in real time with sufficient bandwidth and capacity; dynamically allocate payload, beam, time, and frequency resources to provide real-time access services for massive concurrent users; establish bidirectional TT&C links with more distant deep-space probes; and provide spacecraft positioning, cataloging, collision warning, and other space traffic management services. The main performance indicators are shown in Table 1.

3. System Architecture Design

Considering system reliability, service economy, technical advancement, and feasibility, the system adopts a decentralized, regional cluster-autonomy concept and is designed as a three-layer architecture: a non-geostationary distributed space-based constellation, an integrated space–ground core hub network, and a ground intelligent receiving and processing system.

3.1 Non-Geostationary Distributed Constellation

The constellation deployment, satellite payloads, and onboard switching and processing are designed under requirements for 100% global dual coverage, maximized visibility to cislunar space, and system reliability, as well as engineering constraints such as launch-site location, launch-vehicle drop-zone safety, and low-cost deployment.

3.1.1 Constellation Orbit Design

Design considerations. To obtain global coverage, including polar regions, and to make full use of launch-vehicle capacity under launch-site latitude constraints, the satellites are deployed in IGSO. To reduce launch cost while satisfying drop-zone safety constraints, the orbital inclination is selected so that satellites can be inserted without changing the orbital plane. The number of satellites and orbital parameters are then configured to achieve global coverage and high system robustness.
Design result. Among Chinese launch sites, Xichang is

Table 1: Main performance indicators of the proposed system.

Indicator	**Requirement**
Coverage capability	1. 100% dual coverage of Earth-orbit space below 3000 km; 2. Capability to extend coverage to cislunar space.
Number of users	1. Registered users ≥ 1,000,000 ; 2. Concurrent TT&C users (S/X-band): 100,000; 3. Concurrent data-transmission user (X-band): 3000; 4. Concurrent data-transmission user (QV-band): 6; 5. Concurrent data-transmission user (laser): 12.
Transmission rate	1. S/X-band TT&C: 2 kbps forward and 16 kbps return; 2. X-band data-transmission: 10 Mbps near Earth and 100 kbps in cislunar space; 3. Q/V-band data-transmission: 1 Gbps near Earth and 1 Mbps in cislunar space; 4. Laser links: 5 Gbps near Earth and 100 Mbps in cislunar space.
Feeder-link bandwidth	1. 5 GHz for microwave links; 2. 100 GHz for laser links.
Service response time	1. < 5 s for basic TT&C services; 2. < 10 s for data communication services.
Frequency-band planning	1. S/X bands for TT&C; 2. X, Q/V, and laser for data transmission; 3. Q/V and laser for feeder links.

selected because its higher latitude imposes smaller constraints on orbital inclination design. With a launch-site latitude of 28.2°N, an inclination of 28.5° is selected so that satellites can be inserted without active orbital-plane changes while satisfying drop-zone safety constraints.

Taking advantage of the dynamic characteristic that the IGSO orbital period is synchronous with Earth's rotation period, three uniformly distributed IGSO satellites can provide global coverage. On this basis, six IGSO satellites are adopted to provide global dual coverage.

The six satellites are deployed in three orbital planes away from the lunar orbital plane, so as to maximize geometric visibility to Earth–Moon transfer spacecraft, lunar-orbit satellites, and lunar-surface facilities operating near that plane. Under a "center-free and dual-coverage" concept, the right ascension of the ascending node and true anomaly of the six satellites are configured to avoid system paralysis caused by a single-satellite failure and to ensure stable and reliable links.

Satellite data are mainly returned by direct links to ground stations. When there is no sufficient geographic span to support direct feeder links from all satellites, or if space-to-ground spectrum bandwidth is insufficient for concentrated return of large data volumes, single-hop inter-satellite links may be used for data return. In that case, design backup inter-satellite links to prevent information islands caused by interruption of a unique path.

The resulting non-geostationary distributed space-based constellation architecture is shown in Fig. 1, the constellation orbital parameters are listed in Table 2, and the track of subsatellite point is illustrated in Fig. 2.

3.1.2 Satellite Payload Design

Design considerations. The constellation adopts a decentralized concept in which each satellite carries the same payloads, and mutual backup among satellites improves constellation reliability. A hybrid laser–microwave approach is adopted. Microwave and laser transmission payloads provide differentiated high-rate data services and increase system communication capacity. Space-to-ground feeder links mainly use distributed multi-station laser reception, complemented by microwave links to improve availability under different weather conditions. Higher-frequency Q/V bands are selected for high-rate data transmission to facilitate smaller user terminals at a given data rate.

S/X phased-array antenna. To support diverse on-orbit users while avoiding inter-beam interference, the antenna beamwidth should be as narrow as possible. The prelimi-

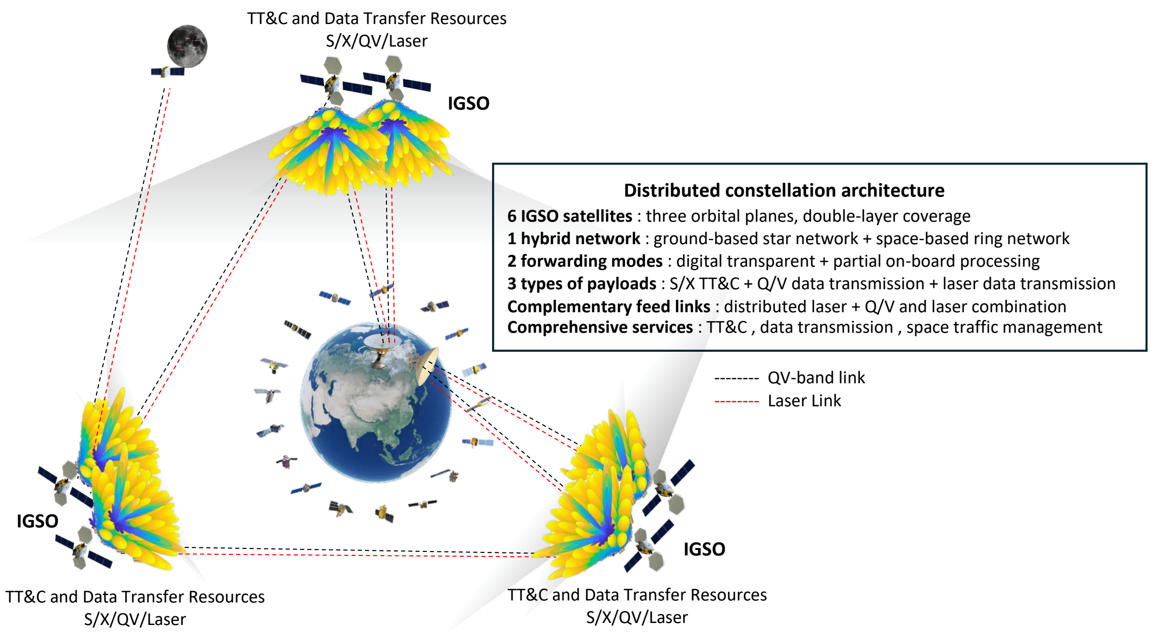

Fig. 1: Non-geostationary distributed space-based constellation architecture.

Table 2: Constellation orbital parameters.

a (km)	e	i (deg)	ω (deg)	Ω (deg)	f (deg)
42166	0	28.5	0	280	300
42166	0	28.5	0	40	60
42166	0	28.5	0	160	300
42166	0	28.5	0	40	180
42166	0	28.5	0	160	60
42166	0	28.5	0	280	180

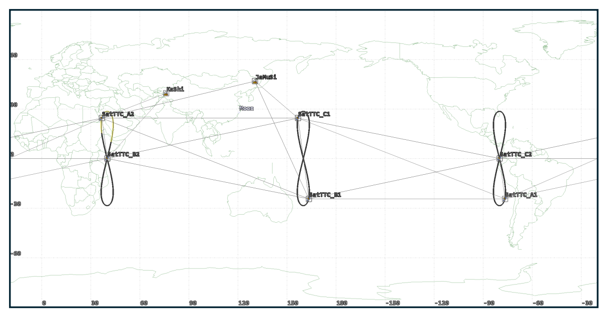

Fig. 2: track of subsatellite point.

nary design adopts a 4 m electrical aperture for the onboard antenna.

The antenna beamwidth variation with pointing angle can be approximately expressed as:

$$\theta = 50.8\frac{\lambda}{D\cos\varphi}, \qquad G(\varphi) = \eta\frac{4\pi D^2}{\lambda^2}\cos^2\varphi. \quad (1)$$

Here, λ is wavelength, D is antenna diameter, η is efficiency, θ is beamwidth, and φ is pointing angle.

For a total scan field of view of 120°, a 4 m aperture antenna corresponds to a single-beam angle of approximately 1.74° in S band and 0.48° in X band. Considering beam-overlap interference, sidelobe interference, signal-to-noise-ratio loss, and engineering constraints to minimize the number of beams and reduce construction cost, the design uses 1024 S-band receive beams and 2048 X-band receive beams.

Based on antenna aperture, scan range, and signal wavelength, and considering engineering constraints such as heat dissipation, the antenna array is designed with 181×181 dual-band radiating elements, 20×20 subarrays, and 9×9 elements per subarray. The radiation unit adopts a multi-layer chip-on-surface design with a common aperture, as well as a hybrid architecture design that combines analog sub-array phase shifting with the back-end digital beamforming. By integrating S-band TT&C and X-band data transmission on a single physical aperture, this design avoids the large volume, high mass, beam-pointing mismatch, and poor platform adaptability of conventional dual-aperture designs. The antenna surface uses a low-expansion carbon-fiber honeycomb sandwich structure, with surface accuracy satisfying X-band radiation requirements (RMS ≤ 2 mm). The achievable normal gain of the antenna is as follows: 38.5 dBi for the S-band and 47.3 dBi for the X-band; the 3 dB beam width is approximately 1.74° for the S-band and 0.48° for the X-band; the scanning losses at 20° and 60° are 0.6 dB and 6.5 dB respectively.

Most user-terminal TT&C antennas provide near-hemispherical (2π steradian) coverage, while some configurations can achieve near-spherical (4π steradian) coverage. The system is designed to schedule antenna beams to cover a specific user simultaneously and perform coherent combination, thereby further reducing user-terminal EIRP and G/T requirements or improving service performance.

Users may also use S/X links as signaling channels to send service requests for additional resources. This is especially important for cislunar user spacecraft at distances roughly ten times greater than near-Earth space. The antenna installed opposing the direction of the satellite's earth-pointing direction provides reduced-rate transmission of key parameters and commands, and at the same time the TT&C link also offers a path for requesting high-rate data resources to obtain more spacecraft status information.

Working with standard civil and commercial user terminals which cover approximately hemispherical (2π steradian) coverage and broadcast telemetry continuously, the onboard phased-array antenna can also obtain one-way pseudorange measurements from user terminals. This enables cataloging of medium-and low-orbit civil and commercial spacecraft and catalog-based collision warning and space traffic management.

Q/V mechanical antenna. To improve data rates, provide differentiated services that complement the satellite internet constellation, and help user satellites reduce antenna size and mass, the system selects Q/V bands for microwave high-rate data transmission services.

According to the communication distance of typical application scenarios, a 2.5 m aperture Q/V antenna is adopted to minimize user-terminal power and size requirements. Considering engineering constraints, implementation difficulty, and economic cost, a rigid umbrella structure compatible with the launch-vehicle fairing in its stowed state is selected. When the transmission power of the Q/V antenna is 20 W, and the aperture of the user spacecraft antenna is 1 m with a transmission power of 10 W, the system meets the carrier-to-noise ratio requirements necessary for 1 Gbps data transmission under the condition of the maximum inter-satellite distance of 44,000 kilometers. When the antenna aperture of the user is 0.4 m, the achievable transmission rate is 150 Mbps.

The Q/V antenna can also be used for space-to-ground feeder links. It complements laser links when atmospheric turbulence causes a sharp increase in bit errors and interrupts optical links. With a 4 dB margin and a ground receiving station antenna larger than 13 m, the Q/V feeder link can reach 5 Gbps, the same rate as the laser feeder link.

Laser terminals. Each satellite carries two 300 mm laser terminals and two 150 mm laser terminals with flexibly adjustable pointing. These terminals support high-rate data transmission for user spacecraft, inter-satellite links for constellation networking, and functional switching and reuse as a weather backup for microwave feeder links.

The 300 mm laser terminals operate with 10–50 mm user terminals in near-Earth space and 100 mm user terminals in cislunar space, mainly providing high-rate data transmission services for user spacecraft. The 150 mm terminals support space-to-ground feeder transmission, establish inter-satellite links for integrated space–ground networking within the constellation, and also provide high-rate data services to users.

When the ground system is operating normally, eight laser terminal resources are used to establish the necessary laser links within the constellation. When ground-system faults prevent downlink through space-to-ground feeder links, the constellation uses 12 laser terminals to build a complete space-based laser network and provides data relay services through direct delivery over a space-based cloud formed by that network.

3.1.3 Onboard Switching and Processing

Design considerations. Data exchange mainly uses transparent forwarding, supplemented by regenerative processing. Considering onboard processing resources are limited and difficult to expand in orbit, transparent forwarding is primarily used, satellites only perform spectrum splitting for radio frequency signals and path routing, as well as beam resource scheduling, without performing demodulation and decoding. To maintain service continuity when the ground system fails, each satellite carries limited processing resources to demodulate, decode, route, and switch data for users with known communication protocols, and delivering data directly to user-specified destinations. The satellites also support signaling processing and some core-network functions, serving as a backup to the ground core network and improving emergency response capability.

Design result. The onboard switching and processing functions support physical-layer transparent forwarding and switching in the digital and analog domains, link-layer and network-layer packet switching under regenerative forwarding, and autonomous onboard processing of signaling and selected core-network functions, as shown in Fig. 3. Transparent forwarding is implemented through digital and analog switching units, regenerative processing and switching is through a high-speed routing unit, and resource scheduling and configuration is through an integrated processing and management unit.

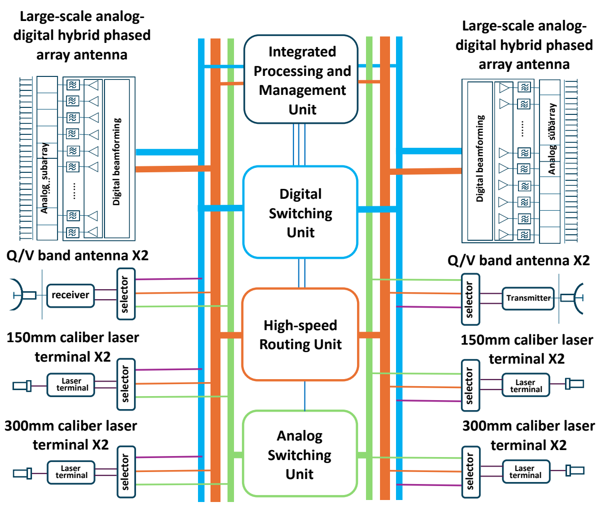

Fig. 3: Onboard switching and processing.

The digital switching unit performs transparent forwarding and switching of digitized user signals in the digital domain, enabling switching among arbitrary beams, frequency bands, and specified time slots. User signals connect to the digital switching unit through the large-scale analog–digital hybrid DBF phased-array antenna link, Q/V antenna link, and laser link.

The analog switching unit performs transparent forwarding and switching of user signals in the analog domain. It switches user signals among multiple Q/V links and laser links across frequency bands, enabling switching among arbitrary beams and frequency bands. Q/V antenna links connect analog-domain signals directly to the analog switching unit, while laser terminals can deliver microwave signals to the analog switching unit during optical mixing.

The high-speed routing unit performs packet switching of user data. It supports link-layer data-frame switching and network-layer IP packet switching. IP packet switching is used for digitized data from Q/V antenna links and laser links, while CCSDS data-frame switching is used for digitized TT&C data from the large-scale analog–digital hybrid DBF phased-array antenna link.

The integrated processing and management unit manages the digital switching unit, high-speed routing unit, and analog switching unit; processes signaling; and implements selected core-network functions such as network management and control, topology routing, and resource scheduling. The system provides full-space coverage through large-scale phased-array antenna beams. User spacecraft access the system through omnidirectional TT&C antennas and submit service requests. The integrated processing and management unit sets a group of fixed signaling frequencies and uses the ALOHA protocol [25] for access, meeting the need for high-value users to request and receive continuous data relay services when the ground system is unavailable.

3.2 Integrated Space–Ground Core Hub Network

Each satellite in the constellation carries processing resources for selected core-network functions. These resources are interconnected and shared through the core hub network, and cloud techniques are used to decouple upper-layer applications from underlying physical facilities [26–28]. The core hub network is carried by inter-satellite laser links and space-to-ground feeder links, enabling unified space–ground scheduling of the constellation's TT&C and data transmission resources.

Under normal conditions, a ground-based star network provides service, and the ground center undertakes core-network functions, performs unified planning and scheduling of space-based TT&C and data transmission resources, and manages user authentication and billing. To improve emergency response capability, the constellation is equipped with selected core-network functions. When ground-center processing resources are unavailable, the system can rapidly switch to a ring network based on a space-based cloud platform to serve users. The integrated core hub network is shown in Fig. 4 and Fig. 5.

3.2.1 Ground-Based Star Network

Each satellite is treated as an autonomous domain. Inter-satellite laser links and space-to-ground feeder links jointly form the bearer network connecting all autonomous domains. To avoid user-data loss caused by short interruptions of inter-satellite or space-to-ground links, hot backup is used to ensure reliability of the star network. Based on the maximum possible number of 100,000 concurrent TT&C users, the access network and data bearer network are designed for traffic matching. In regenerative mode, 1600 Mbit/s of telemetry data traffic is generated. In an

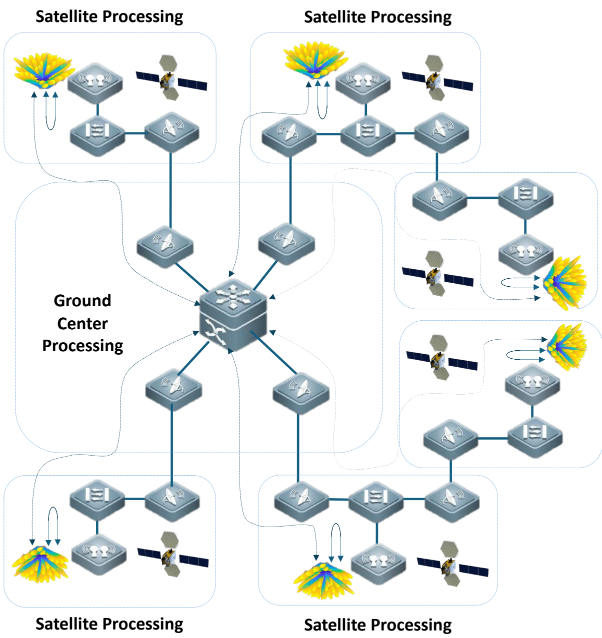

Fig. 4: Ground-Based Star Network.

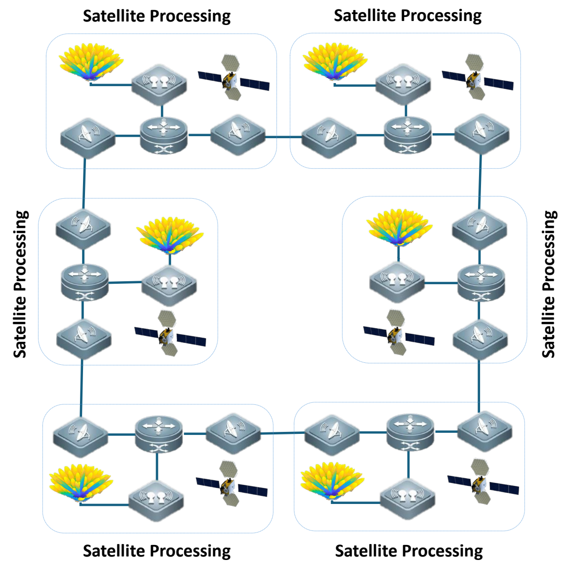

Fig. 5: Space-Cloud-Based Ring Network.

extreme case where data from two satellites are returned through a single feeder link, the satellite-to-ground network bandwidth should reach 3.2 Gbps. In transparent-forwarding mode, each S/X TT&C beam occupies 90 MHz total bandwidth, with another 10 MHz guard band, the space-to-ground link bandwidth should reach 100 GHz when data from 1000 beams are returned simultaneously.

Core-network functions are located at the ground center. The TT&C and data transmission resources provided by the constellation are planned and scheduled by the ground center in an integrated manner. Registered users can randomly submit service requests through TT&C channel and access the ground center through the integrated space–ground network. The ground center authenticates and authorizes users, allocates and schedules resources according to user priority, and performs billing management. After user service data access the satellite through multi-beam antennas, the data can be returned through feeder links and distributed by the ground center to user centers, or switched directly onboard and delivered to user-specified targets according to ground-center configuration information.

3.2.2 Space-Based Cloud Ring Network

In the space-based ring network, inter-satellite laser links form the bearer network connecting all autonomous domains. Because current laser inter-satellite communications still have a probability of random interruptions on the order of seconds, dual-route transmission is adopted to ensure high bearer-network reliability and prevent large-scale user-data loss caused by interruption of any single laser link.

As a backup to the ground core network, the constellation can process signaling and implement selected core-network functions. Satellite processing resources are interconnected and shared through the core hub network, and cloud techniques decouple upper-layer applications from underlying physical facilities. The onboard integrated processing and management unit can process signaling at specified frequency points, perform transparent forwarding, and process application-layer data for special users with known communication protocols, meeting their need for uninterrupted transmission of critical service data.

3.2.3 Switching Between Network Forms

In normal operation, the system works in star-network mode. All satellites in the constellation periodically send network-state monitoring packets, and autonomously switch inter-satellite link connection states according to predefined rules after detecting a star-network failure. When the ground system fails, missions switch to ring-network mode of space-based cloud platform autonomously by satellite. Each satellite uses two 150 mm laser terminals to establish links with two visible satellites, forming a six-satellite ring. The system then operates in a ground-independent space-based ring network, and the constellation assumes selected core-network functions such as user registration management, mobility management, authentication, wireless resource scheduling, switching management, network topology management, and network routing management.

3.3 Ground Intelligent Receiving and Processing System

The ground system adopts a pooled software-defined architecture consisting of antenna units, distributed units, centralized units, and a central-server cloud platform. Distributed and centralized units process data at the signal layer. The central server processes information-layer data, including service functions such as mission planning, resource allocation, and data distribution, as well as core-network functions such as authentication and mobility management.

3.3.1 Antenna Unit

The antenna unit performs radio-frequency signal processing and completes analog-to-digital conversion tasks for Q/V feeder stations and adaptive optical stations. The interface between the antenna unit and the distributed unit is an I/Q digitized bitstream, transmitted over long distances through high-speed optical fiber.

3.3.2 Distributed Unit

The distributed unit performs transparent-forwarding or processing-and-forwarding for user service data. Signaling data are directly passed through the distributed unit to the centralized unit for signal-layer processing.

For users whose TT&C and data-transmission protocols are confidential, the distributed unit performs transparent forwarding. Following the minimum-bandwidth principle, it applies digital-domain filtering and downsampling to bitstreams from ground-system antenna units to separate user frequency bands. If the system is configured for local switching, the data streams are rearranged according to rules and returned to the antenna unit for transmission to the satellite; the satellite then sends them to the corresponding beam to complete data switching, or the data are delivered directly to the user through the ground network. If the system is configured for non-local switching, the bitstream is transmitted to the centralized unit for processing.

For users with known TT&C and data-transmission protocols, processing-and-forwarding can be used. Based on configuration information, the downlinked satellite data are demodulated to obtain the identifier (SCID) of the user spacecraft. If the system is configured for local switching, the user information is appended with the destination beam address and returned to the antenna unit for transmission to the satellite; the satellite sends it to the destination beam according to address configuration, or the data are delivered directly through the ground network. If the system is configured for non-local switching, the demodulated user information is sent to the centralized unit for processing.

3.3.3 Centralized Unit

The centralized unit performs signaling processing, cross-satellite data switching, and cross-region ground data distribution.

For signaling forwarded by the distributed unit, the centralized unit performs demodulation, feature extraction, user fingerprint identification, and other multi-user detection functions, and then sends the results to the central-server cloud platform for authentication, registration, mobility management, and space traffic management.

After cross-satellite data are gathered at the centralized unit, the centralized unit arranges the data according to the system switching table and returns them to the corresponding ground-system antenna units. Cross-region user data are sent to the user center after switching is completed at the centralized unit.

3.3.4 Central-Server Cloud Platform

The central-server cloud platform implements core-network functions such as registration management, authentication, and mobility management, as well as service functions including constellation status monitoring, TT&C resource management, cataloging and warning, and intelligent hosting. It is decoupled from antenna, distributed, and centralized units to facilitate system upgrades. The platform uses multi-site disaster recovery backup to avoid system collapse caused by a single-point failure.

4. System Regime Design

In response to the functional characteristics of the system design, such as massive user simultaneous access, space traffic management based on cataloging, and signal synthesis when user spacecraft are covered by multiple satellites and multiple beams, the technical systems for multi-user access, space traffic management, and multi-beam coherent combination are designed.

4.1 Multi-User Access

The return beams of the satellite phased-array antenna receive service requests sent through USB or UXB user downlink telemetry channels. Different users are identified through a three-dimensional multiple-access regime: spatial multi-beam access, frequency-division multiple access based on the frequency feature differences within the beams, and code-division multiple access, which improves user capacity and meets the requirement for massive simultaneous access.

4.1.1 Frequency Division Multiplexing Based on Frequency Feature Differences

Because different users have different relative motion with respect to the relay satellite and different oscillator characteristics, the frequency received by the relay satellite differs from the theoretical value. Therefore, a new frequency-division regime based on frequency-characteristic differences, using frequency and frequency-rate differences as fingerprint information to identify different users, is proposed.

The fractional Fourier transform (FRFT) [29] is used to detect and separate weak linear frequency-modulated signals under low signal-to-noise ratio:

$$X_\alpha(u) = \mathcal{F}_\alpha\{x(t)\} = \int_{-\infty}^{+\infty} K_\alpha(t,u)x(t)\,dt. \quad (2)$$

Among them, the transformation function is:

$$\begin{aligned} K_\alpha(t,u) = &\sqrt{\frac{1-j\cot\alpha}{2\pi}} \\ &\times \exp\left[j\left(\frac{t^2+u^2}{2}\cot\alpha - tu\csc\alpha\right)\right]. \end{aligned} \quad (3)$$

The physical essence of the FRFT is a Fourier transform after arbitrary rotation in the time–frequency plane. When the chirp rate k of the user signal is $-\cot\alpha$, two-dimensional energy concentration is achieved.

For users adopting USB or UXB, the system's dual-coverage design ensures that if frequency-characteristic differences relative to one satellite are too small for separation, the differences relative to another satellite will be large. Therefore, the frequency-division design in which multiple users reuse one frequency point is feasible.

4.1.2 Multiple-Access Regime Combining Spreading Code and Frequency Domain

For users adopting spread-spectrum, user identification can be extended from a single code-domain dimension to a combination of spreading-code domain and frequency-characteristic domain. When frequency characteristics are close, different spreading codes distinguish users. When frequency characteristics differ, the FRFT algorithm selects the optimal rotation angle and separates users in the fractional domain.

4.1.3 Spatial Division Multiplexing Based on Multi-beam

The S/X phased-array antenna supports simultaneous multi-beam reception through 1024 S-band beams and 2048 X-band beams, far exceeding the multi-beam capability of traditional mechanical antennas and supporting concurrent access by more users. Beam hopping with time-division coverage can further expand user capacity. The polling cycle for any spatial region should be as short as possible. The design aims to establish a reliable link with the operator within 5 s when a user is in an abnormal attitude, satisfying the requirement for rapid operator intervention and emergency response after service interruption caused by spacecraft failure.

4.2 Space Traffic Management

By using telemetry signals continuously broadcast by user satellites, the system can locate and catalog user spacecraft and provide collision-avoidance warnings based on catalog information, thereby extending the system to space traffic management.

Commercial spacecraft generally use USB/UXB TT&C. For registered users, bidirectional measurement information can be used for orbit determination. For unregistered users, one-way measurements can be used, but localization accuracy based only on telemetry signals is limited, therefore the user terminal must additionally broadcast DOR ranging tones, namely:

$$s_t(t) = A_c\cos(\omega_c t) + \sum_{k=1}^{N} m_k\cos(\omega_k t) + m_Y s_Y(t). \quad (4)$$

Here, m_k is the modulation index of the kth DOR ranging tone, ω_k is the angular frequency of the ranging tone, $m_Y s_Y(t)$ is the telemetry subcarrier signal, A_c is the signal amplitude, and $s_t(t)$ is the telemetry signal.

Real-time positioning can be achieved when four satellites with good geometry receive DOR ranging tones. Otherwise, long-duration multi-satellite measurements are required for orbit determination.

For a single satellite, at the user transmission time τ_u, the phase of each ranging tone is $\phi_k(\tau_u) = \omega_k\tau_u$. After satellite i locks onto the user's DOR ranging tone, the reproduced ranging-tone phase is the user transmission phase plus the phase lag introduced by propagation, $\phi_{k,s_i}(\tau_{s_i}) = \omega_k(\tau_u - \Delta\tau_{s_i})$. Because there is a time-frequency offset δt between the satellite and the user, the phase-difference measurement obtained by the satellite using its local frequency reference can be written as:

$$\Delta\phi_{k,s_i} = \mathrm{mod}\left(\omega_k \Delta\tau_{s_i} + \delta t, 2\pi\right). \quad (5)$$

By jointly using multiple ranging tones, the integer ambiguity of range can be obtained, and the pseudorange measurement can then be derived as:

$$\rho_i = \sqrt{(x_{s_i} - x_u)^2 + (y_{s_i} - y_u)^2 + (z_{s_i} - z_u)^2} + c\delta t. \quad (6)$$

Here, ρ_i is the pseudorange measurement, c is the speed of light, $(x_{s_i}, y_{s_i}, z_{s_i})$ is the position of the ith satellite, and (x_u, y_u, z_u) is the user position.

The satellite constellation keeps time using high-precision atomic clocks and performs time synchronization. Pseudorange measurements from multiple satellites form simultaneous equations from which the user's three-dimensional position and clock offset can be solved:

$$\begin{aligned}
\sqrt{(x_{s_1} - x_u)^2 + (y_{s_1} - y_u)^2 + (z_{s_1} - z_u)^2} &= \rho_1 - c\delta t, \\
\sqrt{(x_{s_2} - x_u)^2 + (y_{s_2} - y_u)^2 + (z_{s_2} - z_u)^2} &= \rho_2 - c\delta t, \\
\sqrt{(x_{s_3} - x_u)^2 + (y_{s_3} - y_u)^2 + (z_{s_3} - z_u)^2} &= \rho_3 - c\delta t, \\
\sqrt{(x_{s_4} - x_u)^2 + (y_{s_4} - y_u)^2 + (z_{s_4} - z_u)^2} &= \rho_4 - c\delta t.
\end{aligned} \quad (7)$$

When the number of users is large, user carriers and DOR ranging tones may be multiplexed within an antenna beam. The system then uses the SCID in telemetry frames to identify users and avoid mismatching DOR ranging-tone data from different users observed at different times.

In real-time positioning, user time-frequency performance does not affect the positioning result. When multiple arcs are used for orbit determination, however, the clock offset must be treated as a time variable, and the three coefficients in the quadratic clock model $a_0 + a_1(t - t_0) + a_2(t - t_0)^2$ must be solved. Because clock stability affects the fitting error of the quadratic function, the coefficients must be re-estimated by segments, with segment length determined by the clock performance selected by each user.

According to the orbital dynamics of the designed constellation, every LEO user has arcs that satisfy real-time positioning conditions and arcs that require long-duration measurements for orbit determination. Taking the user clock offset obtained from real-time positioning as the initial value, user position information can be obtained through orbit determination using continuous pseudorange measurements acquired from constellation reception of DOR ranging tones and telemetry information.

For spacecraft adopting spread-spectrum, the telemetry signal spectral density is very low, and matched filtering cannot be performed when the spreading-code sequence is unknown. Therefore, positioning of spread-spectrum users requires public disclosure of their spreading-code sequences. The system assigns different initial phases to different users and then performs despreading and measurement, extracts the SCID from telemetry frames to identify the spacecraft, and determines the user orbit in the same way as for USB and UXB users.

To prevent users from forging SCIDs to evade control, the system must have user-fingerprint identification capability. Unique physical characteristics carried by the radio-frequency signals emitted by user spacecraft, such as phase noise and spectral features, can usually be served as fingerprint information.

4.3 Multi-Beam Coherent Combination

4.3.1 Theoretical Analysis

After the telemetry signal of the same user is received by multiple beams, coherent combination through phase-difference search can accumulate energy and enable reception of weaker signals. The system therefore further reduces user-terminal requirements through multi-beam coherent combination.

Inter-beam phase differences are mainly caused by path differences among beams, generally include differences in the space propagation path, analog subarray phase-shifting array, and digital processing.

For overlapping coverage by beams from different satellites, correcting the spatial-propagation phase difference introduces position-uncertainty errors from two satellites. GNSS-based satellite orbit accuracy is on the order of 10 m, and the corrected phase residual remains large relative to the carrier wavelength. In addition, different relative motion and time-frequency differences between satellites introduce frequency-characteristic biases. Coherent combination would require frequency correction including both frequency offset and frequency-rate offset, which is extremely difficult to implement. Therefore, this system design does not consider beam combination under overlapping coverage by beams from different satellites.

For multiple beams from the same phased-array antenna, the space propagation path is the same, and satellite position uncertainty is a common-mode error. Phase differences among multiple beams can therefore be completely eliminated, leaving the phase bias introduced by different analog subarrays as the main error source. The fixed phase delay introduced by different weighting coefficients in the analog subarray phase-shifting array can be calculated, but discrete errors, temperature drift, amplitude-phase distortion, and other factors cause deviations between the calculated result and the actual condition.

When digital-domain beamforming is processed on the same digital platform, phase bias introduced by different beam weighting coefficients can be eliminated by calculation. Systematic time-delay bias caused by different logical units and non-uniform internal chip layout and routing can be eliminated through calibration, but residual errors may still arise from chip-clock changes caused by different operating temperatures.

Therefore, the actual phase difference among multiple beams cannot be obtained accurately through theoretical calculation, and blind coherent combination is required. When multiple receive beams with overlapping spatial coverage receive the same target signal simultaneously and the clocks of the multiple signal paths share the same source, the digital domain can search across the phase-uncertainty range. Using the combined output signal-to-noise ratio or FRFT detection peak as the objective function, the optimal compensation phase is found and the phases of multiple signals are aligned.

Because inter-beam delay differences often contain multiple carrier phase cycles, searching only in the hemispherical (2π steradian) coverage space can easily converge to an incorrect integer-cycle point, seriously degrading coherent-combination gain during telemetry data processing. The ambiguity can then be resolved using telemetry subcarrier phase information carried by the TT&C signal.

4.3.2 Implementation Method

An arbitrary beam signal $s_i(t)$ can be expressed in complex form as:

$$s_i(t) = A_i e^{j[\omega_c t + \phi_{c_i} + \phi_{cd}(t)]} \times e^{j m_y \cos[\omega_y t + \phi_{y_i} + \phi_{yd}(t)]}. \quad (8)$$

Here, A_i is the signal amplitude. The carrier frequency ω_c, subcarrier frequency ω_y, carrier Doppler $\phi_{cd}(t)$, subcarrier Doppler $\phi_{yd}(t)$, and modulation index m_y are the same for any beam signal. As long as the same local oscillator is used in multi-beam signal processing, no new phase bias is introduced. However, the carrier phase shift ϕ_{c_i} and subcarrier phase shift ϕ_{y_i} differ among beam signals, and the inter-signal deviations must be estimated.

Typically $m_y \ll 1$, so:

$$s_i(t) \approx A_i e^{j[\omega_c t + \phi_{c_i} + \phi_{cd}(t)]} \times \left\{1 + m_y \cos[\omega_y t + \phi_{y_i} + \phi_{yd}(t)]\right\}. \quad (9)$$

Multi-beam coherent combination is implemented in three steps. First, blind deviation search is performed on carrier signals received by multiple beams to achieve coherent combination and acquisition. After stable carrier lock, the main carrier is stripped from each received beam signal, and a second blind search is performed at the subcarrier level for coherent combination, compressing the delay-ambiguity interval and completing subcarrier loop lock. Finally, a third coherent combination is performed on telemetry data bits to complete demodulation.

Because coherent combination is performed at three levels, the blind-search space grows cubically with the number of beams. From the perspective of algorithmic resource consumption, this method is therefore only suitable when the number of overlapping beams is small. When more than four beams are combined, the time-delay uncertainty must be substantially compressed and the phase-search space reduced. In engineering implementation, delay-difference tests should also be conducted before antenna delivery under the same pointing direction, possible coverage space, and different high- and low-temperature environments. These tests establish a correction model and obtain the maximum corrected delay variation range. The maximum allowable processing duration should also be determined according to the minimum dwell time of the target within the beam, so that appropriate multi-beam coherent-combination processing resources can be configured.

5. Conclusion

This paper proposes a concept for an IGSO-based space data transmission system. It designs a three-layer architecture consisting of a six-satellite constellation distributed in three orbital planes, an integrated space–ground core hub network combining a ground-based star network and a space-based cloud ring network, and a ground intelligent receiving and processing system. It proposes three categories of service payloads, namely S/X basic TT&C, Q/V medium-rate data transmission, and laser high-rate data transmission; two satellite processing and forwarding modes, namely fully digital transparent forwarding and onboard processing; and complementary feeder links formed by multi-site distributed laser channels and hybrid laser–microwave links. It also designs a three-dimensional multiple-access system based on frequency-characteristic differences, code division, and space division; a positioning and orbit-determination system that uses user-spacecraft telemetry signals for cataloging; and a multi-beam coherent combination system based on blind coherent combination.

The designed system can provide 100% dual coverage for Earth orbits below 3000 km and can extend TT&C and data transmission services to cislunar space. It supports registration of one million spacecraft and real-time online concurrency for 100,000 TT&C channels. It meets the basic TT&C requirements of massive users for routine status monitoring and emergency response under failure conditions, as well as the high-rate data transmission requirements of remote sensing satellites, scientific experiment satellites, and crewed spacecraft. The infrastructure formed during the system construction can also be reused for user-spacecraft positioning, laying the foundation for catalog-based space traffic management.

References

[1] Andrea Modenini and Barbara Ripani. A tutorial on the tracking, telemetry, and command (tt&c) for space missions. *IEEE Communications Surveys & Tutorials*, 25(3):1510–1542, 2023.

[2] Yafeng Zhan, Peng Wan, Chunxiao Jiang, Xiaohan Pan, Xi Chen, and Song Guo. Challenges and solutions for the satellite tracking, telemetry, and command system. *IEEE Wireless Communications*, 27(6):12–18, 2020.

[3] D.L. Brandel, W.A. Watson, and A. Weinberg. NASA's advanced tracking and data relay satellite system for the years 2000 and beyond. *Proceedings of the IEEE*, 78(7):1141–1151, 1990.

[4] George Haddad, Thomas Kacpura, James Nessel, Phillip Paulsen, Jonathan Drexler, Eric Hartman, Jeffrey Hayes, and Patrick Boldosser. Framework for NASA Space Relay Satellite Services Over the Next Decade:"Development and Demonstration of the Commercial Successors to TDRS. In *27th Ka and Broadband Communications Conference (Ka) and the 39th International Communications Satellite Systems Conference (ICSSC)*, 2022.

[5] Caiyu Liu and Yao Wu. History and trends in the development of low-orbit satellite communication systems. In *2024 IEEE 24th International Conference on Communication Technology (ICCT)*, pages 1044–1048, 2024.

[6] Harald Hauschildt, Silvia Mezzasoma, Hermann Ludwig Moeller, Michael Witting, and Jörg Herrmann. European data relay system goes global. In *2017 IEEE International Conference on Space Optical Systems and Applications (ICSOS)*, pages 15–18, 2017.

[7] C.-H. Rokitansky, M. Ehammer, and Th. Graupl. Communication capacity assesment for the iris satellite system. In *2008 IEEE/AIAA 27th Digital Avionics Systems Conference*, pages 2.B.3–1–2.B.3–13, 2008.

[8] Alen Luštica, Sanja Šamanović, Domagoj Frank, and Olga Bjelotomić Oršulić. Data transmission technologies and relay systems in the copernicus sentinel program. In *2025 International Symposium ELMAR*, pages 239–244. IEEE, 2025.

[9] Rui Li, Baojun Lin, Yingchun Liu, Mingji Dong, and Shuai Zhao. A survey on laser space network: Terminals, links, and architectures. *IEEE Access*, 10:34815–34834, 2022.

[10] Shane Laverty, Wen Cheng Chong, Jeffrey Osborne, Mina Mitry, and Vanessa Lewis. *The Kepler Satellite System*, pages 1075–1090. Springer International Publishing, Cham, 2020.

[11] Gao Yuxuan, Li Yue, and Shi Penghui. Research status of typical satellite communication systems. In *2021 19th International Conference on Optical Communications and Networks (ICOCN)*, pages 1–3. IEEE, 2021.

[12] Guodong Tan, Qunbiao Wang, Xuechao Duan, Dongwu Yang, Shufei Feng, and Guangda Chen. Rapid optimization of feed location for high-gain umbrella-type antennas via heuristic electromechanical coupling. *IEEE Transactions on Antennas and Propagation*, 73(10):7260–7274, 2025.

[13] Xiaoyu Hong, Weiren Wu, Qinghui Liu, Dengyun Yu, Chi Wang, Tao Shuai, Weiye Zhong, Renjie Zhu, Yonghui Xie, Lihua Zhang, Liang Xiong, Yuhua Tang, Yongliao Zou, Haitao Li, Guangli Wang, Jianfeng Xie, Changbin Xue, Hao Geng, Juan Zhang, Xiaojing Wu, Yong Huang, Weimin Zheng, Lei Liu, Fang Wu, Xiuzhong Zhang, Tao An, Xiaolong Yang, Fengxian Tong, Leonid I. Gurvits, Yong Zheng, Minfeng Gu, Xiaofei Ma, Liang Li, Peijia Li, Shanshan Zhao, Ping Rui, Luojing Chen, Guohui Chen, Ke Li, Chao Zhang, Yuanqi Liu, Yongchen Jiang, Jinqing Wang, Wenbin Wang, Yan Sun, Longfei Hao, Lang Cui, Dongrong Jiang, Zhihan Qian, and Shuhua Ye. Lunar orbital VLBI experiment: Motivation, scientific purposes and status. *Science China Physics, Mechanics & Astronomy*, 69(1):219511, 2025.

[14] Sami Ma, Yi Ching Chou, Haoyuan Zhao, Long Chen, Xiaoqiang Ma, and Jiangchuan Liu. Network Characteristics of LEO Satellite Constellations: A Starlink-based Measurement from End Users. In

Ieee INFOCOM 2023-IEEE Conference on Computer Communications, pages 1–10. IEEE, 2023.

[15] Nils Pachler de la Osa. *Optimizing resource allocation in large communications satellite constellations*. PhD thesis, Massachusetts Institute of Technology, 2024.

[16] A Le Kernec, L Canuet, A Maho, M Sotom, D Matter, and L Francou. Optical feeder links for high throughput satellites and the H2020 VERTIGO project. In *COAT-2019 - workshop (Communications and Observations through Atmospheric Turbulence: characterization and mitigation)*, Châtillon, France, December 2019. ONERA.

[17] Jiasheng Wang and Xin Qi. China's data relay satellite system served for manned spaceflight. *SCIENTIA SINICA Technologica*, 44(3):235–242, 2014.

[18] Chunlai Li, Jianjun Liu, Xin Ren, Wei Zuo, Xu Tan, Weibin Wen, Han Li, Lingli Mu, Yan Su, Hongbo Zhang, Jun Yan, and Ziyuan Ouyang. The Chang'e 3 Mission Overview. *Space Science Reviews*, 190(1):85–101, July 2015.

[19] Peng Zhang, Wei Dai, Ran Niu, Guang Zhang, Guanghui Liu, Xin Liu, Zheng Bo, Zhi Wang, Haibo Zheng, Chengbao Liu, Hanzhe Yang, Yifan Bai, Yang Zhang, Dong Yan, Kefa Zhou, and Ming Gao. Overview of the Lunar In Situ Resource Utilization Techniques for Future Lunar Missions. *Space: Science & Technology*, 3:0037, 2023.

[20] Shaojun Bi, Changgang Zheng, Congwei Yang, Jinjun Zheng, Chengyan He, and Jiaxing Liu. In-orbit Experimental of Satellite-induced Code Pseudorange Deviations of BeiDou System. In *Proceedings of the 31st International Technical Meeting of the Satellite Division of the Institute of Navigation (ION GNSS+ 2018)*, pages 1257–1267, Miami, Florida, USA, September 2018. Institute of Navigation.

[21] Yun Liu and Yangting Lin. Key Scientific Questions for Future Lunar Exploration. *Space: Science & Technology*, 4:0241, 2024.

[22] Steve Creech, John Guidi, and Darcy Elburn. Artemis: An Overview of NASA's Activities to Return Humans to the Moon. In *2022 IEEE Aerospace Conference (AERO)*, pages 1–7, 2022.

[23] Helena Zofia Tataj, Jasmin della Guardia, and Bernard Foing. Experience of Reality, Stressors, and NPS in All-Female Analogue Lunar Base Crews. *Space: Science & Technology*, 0(ja).

[24] Bill Stockman, Joe Boyle, and John Bacon. International Space Station Systems Engineering Case Study. Systems Engineering Case Study NASA/SP-2007-6105, National Aeronautics and Space Administration, 2010.

[25] Richard T. B. Ma, Vishal Misra, and Dan Rubenstein. An analysis of generalized slotted-aloha protocols. *IEEE/ACM Trans. Netw.*, 17(3):936–949, June 2009.

[26] Changgang Zheng, Bowen Yang, Jin Ke, Ye Yang, Enge Song, Haonan Li, Zihao Fan, Mingxin Li, Yilong Lv, Yisong Qiao, Jun Liang, Donglin Lai, Bengbeng Xue, Yang Song, Xing Li, Rong Wen, Zhigang Zong, and Shunmin Zhu. Single-Core Hotspots on Your VNF? Break Them Up! In *Proceedings of the 10th Asia-Pacific Workshop on Networking*, APNet '26, Singapore, Singapore, August 2026. Association for Computing Machinery.

[27] Haonan Li, Tian Pan, Jin Ke, Baohai Hu, Changgang Zheng, Enge Song, Zhi Xu, Ye Yang, Bowen Yang, Donglin Lai, Yisong Qiao, Bengbeng Xue, Jianyuan Lu, Xiaoqing Sun, Shize Zhang, Zihao Fan, Mingxin Li, Yang Song, Jun Liang, Xionglie Wei, Biao Lyu, Rong Wen, Zhigang Zong, Jiao Zhang, Tao Huang, and Shunmin Zhu. CStar gateway: Augmenting public cloud infrastructure for heterogeneous network function virtualization. In *23rd USENIX Symposium on Networked Systems Design and Implementation (NSDI 26)*, pages 1501–1515, Renton, WA, May 2026. USENIX Association.

[28] Zihao Fan, Xing Li, Ye Yang, Bo Jiang, Bowen Yang, Yilong Lv, Yuke Hong, Yinian Zhou, Junnan Cai, Jiayue Xu, Yunrui Hu, Zhao Gao, Ke Sun, Yimin Liu, Xiangdong Zhang, Enge Song, Jianyuan Lu, Xiaoqing Sun, Shize Zhang, Haonan Li, Mingxin Li, Changgang Zheng, Yang Song, Jun Liang, Biao Lyu, Rong Wen, Zhigang Zong, and Shunmin Zhu. Bifrost: Alibaba's Next-Generation VPC Network with High-Performance Multipath Reliable Transport. In *23rd USENIX Symposium on Networked Systems Design and Implementation (NSDI 26)*, pages 571–590, Renton, WA, May 2026. USENIX Association.

[29] Haldun M Ozaktas and M Alper Kutay. The fractional Fourier transform. In *2001 European Control Conference (ECC)*, pages 1477–1483. IEEE, 2001.